

PAC49 Jeopardy Update for E12-11-009  
The Neutron Electric Form Factor  
at  $Q^2$  up to  $7(\text{GeV}/c)^2$  from the Reaction  ${}^2\text{H}(\vec{e}, e'\vec{n}){}^1\text{H}$   
via Recoil Polarimetry

Revised: 04 July 2021

J.R. Arrington<sup>a</sup>, M. Kohl<sup>b,d</sup>, B. Sawatzky<sup>b,\*</sup>, A. Semenov<sup>c,e</sup>, W. Tireman<sup>f</sup>

<sup>a</sup>*Lawrence Berkeley Laboratory, Berkeley, CA 94720, USA*

<sup>b</sup>*Thomas Jefferson National Accelerator Facility, Newport News, VA 23606, USA*

<sup>c</sup>*JINR, Dubna, Moscow Region, Russia*

<sup>d</sup>*Hampton University, Hampton, VA 23669, USA*

<sup>e</sup>*University of Regina, Regina, SK S4S 0A2, Canada*

<sup>f</sup>*Northern Michigan University, Marquette, MI 49855, USA*

## 1. Introduction

E12-11-009 (“C-GEN”) [1] is a measurement of the neutron electric form factor ( $G_E^n$ ) at nominal  $Q^2$  values of 3.95 and 6.88  $(\text{GeV}/c)^2$  using the reaction  ${}^2\text{H}(\vec{e}, e'\vec{n}){}^1\text{H}$  via recoil polarimetry. Initially proposed at PAC34, it was formally approved in PAC37 [2] with a slight reduction of the requested beamtime, and encouragement to focus on two measured points, one slightly lower than the proposed 3.95  $(\text{GeV}/c)^2$  to better overlap the E02-013 polarized- ${}^3\text{He}$   $G_E^n$  value [3], and then focus the remaining beamtime on the largest accessible  $Q^2$  point.

Section 2 will outline some significant theoretical and experimental developments in the period since PAC37 and demonstrate the continued importance of this measurement. There is significant interest and importance in measuring  $G_E^n$  using the recoil polarimetry technique to compliment and cross-check the upcoming polarized- ${}^3\text{He}$  measurement in Hall A (E12-09-016) [4]. One only has to look the JLab  $G_E^p$  measurements to see the value in using different techniques to access the same quantities [5] in this largely unexplored region.

Section 3 outlines the Collaboration’s activity on E12-11-009 and the very important pause over the last few years as we shifted gears in a joint effort to explore a novel charge-exchange approach to recoil neutron polarimetry outlined by Annand *et. al* in LOI12-15-003 [6]. That new method is described further in Section 3 and will be tested in the exploratory “RP-GEN” (E12-17-004) measurement, approved to run with the SBS program in Hall A this fall (2021). The outcome of that measurement is expected to directly influence the final polarimeter design for any future recoil polarimetry experiment, and may allow that technique to be extended to  $Q^2$  as high as 10  $(\text{GeV}/c)^2$ .

## 2. Motivation

Rationale for measuring  $G_E^n$  was revisited as part of the RP-GEN PAC47 proposal [7] noted above. A number of newer developments outlined in that document are reproduced

---

\*Corresponding author

below.

One of the critical factors driving progress in understanding nucleon structure is the availability of high precision electron scattering results over a broad range of  $Q^2$ . The higher  $Q^2$  domain is relatively unexplored, especially for the neutron, and thus has immense potential to discriminate between different nucleon structure models. Elastic form factors remain a major source of information about quark distributions at small transverse distance scales and the  $Q^2$  dependence of  $G_E^p/G_M^p$  has generated more theoretical papers than any other result to come out of Jefferson Laboratory (JLab). There is considerable anticipation regarding new results that push both  $G_E^p/G_M^p$  and  $G_E^n/G_M^n$  to higher values of  $Q^2$ .

The primary motivation for this proposed experiment is the ability to measure a fundamental quantity of the neutron—one of the basic building blocks of matter. A successful model of confinement must be able to predict both neutron and proton electromagnetic form factors simultaneously. The neutron electric form factor is especially sensitive to the nucleon wave function, and differences between model predictions for  $G_E^n$  tend to increase rapidly with  $Q^2$ . Calculations and fits to the data up to  $1.45 \text{ (GeV/c)}^2$  show significant quantitative differences in the few  $(\text{GeV/c})^2$  range, and make qualitatively different predictions for the behavior of  $G_E^n$  at higher  $Q^2$  values, with some showing  $G_E^n$  falling off more slowly than  $G_M^n$ , and others showing  $G_E^n$  falling rapidly to zero and becoming negative. The proposed measurements of  $G_E^n$  will be able to challenge theoretical calculations, including both models and new rigorous lattice QCD calculations, with a focus on the high  $Q^2$  range where the models of the nucleon are generally meant to be more complete. The sensitivity of this ratio to details of the neutron substructure, and the broad spread in theoretical predictions to those details are demonstrated in Figure 1.

In this ratio technique, systematic uncertainties are extremely small because the analyzing power of the polarimeter cancels in the ratio, and sensitivity to the beam polarization is reduced because it depends only on the small drift in polarization between sequential measurements. Use of a deuteron target yields a better separation between quasielastic and inelastic events, as well as a smaller proton background which must be cleanly separated from the neutron scattering events. Finally, the reaction mechanism and nuclear physics corrections (for FSI, MEC, and IC)] are best understood and can be most reliably corrected for in the deuteron. The combination of these advantages is what yields 2–3% systematic uncertainties for the recoil polarization measurement, while the polarized  $^3\text{He}$  measurements typically have  $\approx 10\%$  systematic uncertainties.

### 2.1. Dyson Schwinger Equation Framework

One particular theoretical technique has come to prominence in the past decade. It is based on the infinite series of Dyson-Schwinger Equations (DSE) that interrelate the Green's functions of QCD [8]. Recent calculations explicitly describe the dynamical generation of the mass of constituent quarks, and show excellent agreement with available lattice QCD results. Using the dressed quarks as the elementary degrees of freedom, the nucleon form factors may be calculated using a Poincaré covariant Faddeev equation (DSE/F) [9]. While still an approximation, the DSE/F approach is based on first principles. It is limited, however, in that precisely three constituent quarks are considered, so that for instance pion-cloud effects are not investigated. However, it is reasonable to assume the dominance of the 3-quark component of the wave function at relatively high values of  $Q^2$ .

Building on the work of Ref. [9] a unified study of nucleon and  $\Delta$  elastic and transition form factors has recently been made [10], which provides (Fig. 2) a consistent description of both  $\mu_p G_E^p/G_M^p$  and  $\mu_n G_E^n/G_M^n$  and predicts for both a zero-crossing point. The location

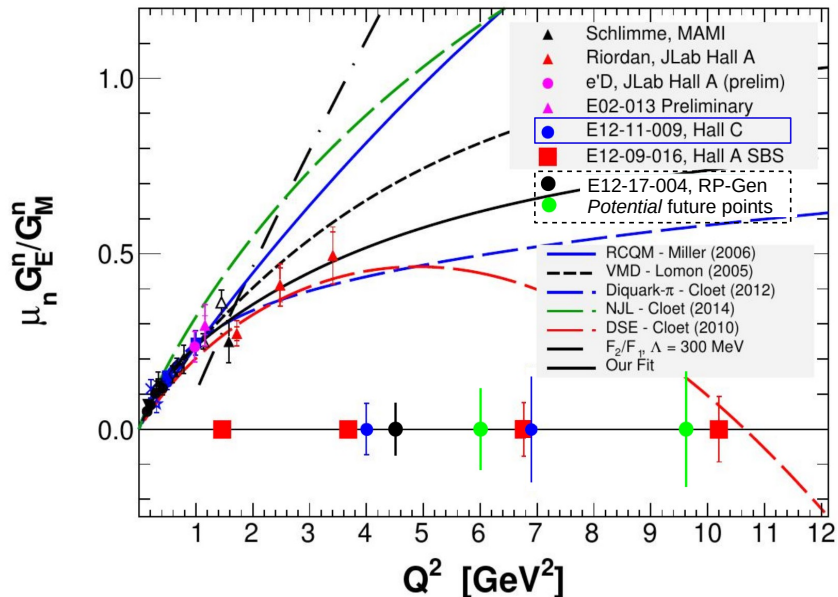


Figure 1: A comparison of projected uncertainties for upcoming  $G_E^n/G_M^n$  measurements. Blue circles reflect the E12-11-009 (C-GEN) proposal [1] projections that do not include sensitivity to the charge-exchange channel. Red squares are for the upcoming SBS polarized  ${}^3\text{He}$   $G_E^n$  measurement E12-09-016 [4]. The black circle reflects the “proof-of-principle” RP-Gen [7] measurement. The green data points reflect uncertainties achievable *if* the charge-exchange recoil polarimetry channel proves viable. Data from the RP-Gen measurement will be used to study extensions to the C-GEN polarimeter to enhance its sensitivity to this reaction channel.

of the zero crossing point (if it exists) of the ratios has implications for the location and width of the transition region between constituent- and parton-like behavior of the dressed quarks. A more rapid transition from non-perturbative to perturbative behavior pushes the proton zero point to higher  $Q^2$ , while conversely the neutron zero point is pushed to lower  $Q^2$ . Thus the ability of the JLab electromagnetic form factor (EMFF) measurements to push into the  $Q^2 \approx 10 (\text{GeV}/c)^2$  domain will have a major impact in testing theoretical predictions of this type. In the case of the neutron the kinematic region of interest is completely unexplored. Within the framework of Ref. [10] di-quark correlations are behind the zero-crossing behavior of  $G_E/G_M$ .

## 2.2. Nambu–Jona-Lasinio Model

Flavor-separated scaling behavior is addressed in Ref. [10] and also in a calculation made within the framework of a covariant, confining Nambu–Jona-Lasinio (NJL) model [19]. For  $F_1$  the dominance of the u-quark sector is interpreted as a consequence of scalar di-quark correlations, which play a smaller role in the  $d$ -quark sector. The  $u$ - $d$  difference for  $F_2$  is less dramatic, due to axial-vector diquark and pion-cloud contributions to the  $d$  sector, counteracting the effect of the scalar di-quark correlation. The comparison with data is limited to  $Q^2 \leq 3.4 (\text{GeV}/c)^2$ , above which there are no data on  $G_E^n$ . Precise new neutron data at  $Q^2 > 3.4 (\text{GeV}/c)^2$  and confirmation of the behavior at  $1.5 > Q^2 > 3.5 (\text{GeV}/c)^2$  are required to further test these new theoretical developments.

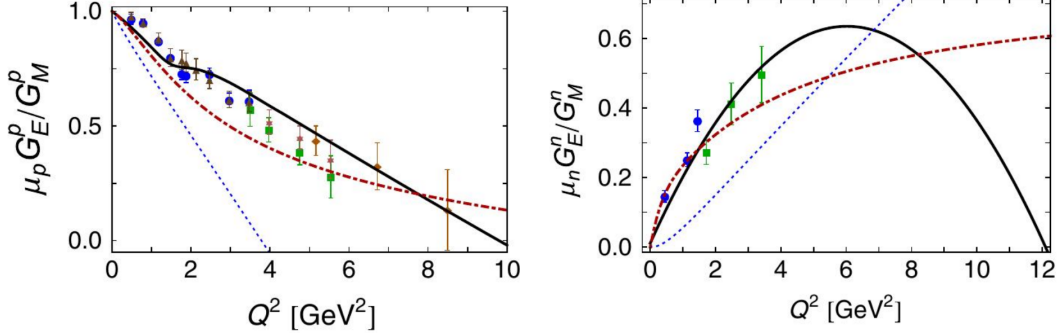


Figure 2: **Left:** “QCD-kindred” calculation [10] (black line) of  $\mu_p G_E^p / G_M^p$  compared to JLab data [5, 11, 12, 13, 14] **Right:** equivalent calculation of  $\mu_n G_E^n / G_M^n$  (black line) compared to JLab. data [3, 15]. Red dot-dash lines are from Ref. [16], and blue dotted lines from Ref. [17].

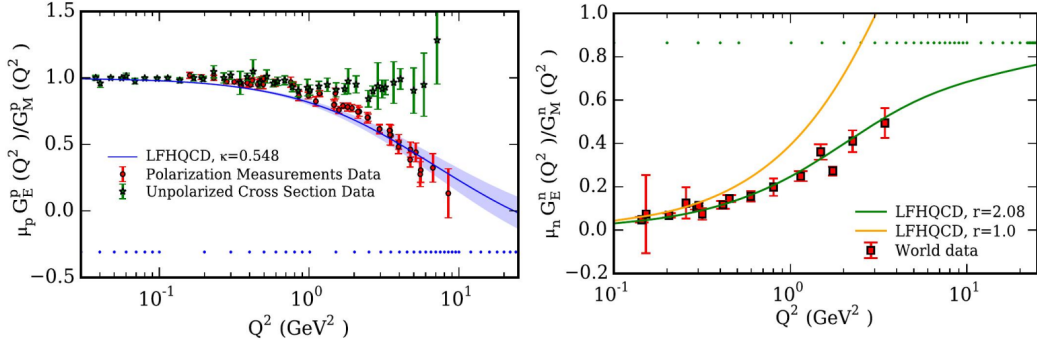


Figure 3: Predictions of Light Front Holographic QCD [18] for the ratios of  $G_E^p / G_M^p$  (left) and  $G_E^n / G_M^n$  (right).

### 2.3. Light Front Holographic QCD

A recent analysis of the nucleon EMFF has been made within the framework of light-front holographic QCD (LFHQCD) [18]. The helicity-conserving and helicity-flip current matrix elements required to compute  $F_1(Q^2)$  and  $F_2(Q^2)$ , have an exact representation in terms of the overlap of the nonperturbative hadronic light-front wave functions and the eigen-solutions of the QCD light-front Hamiltonian. As well as elastic form factors, this framework is also capable of predicting hadronic transition form factors, structure functions and the mass spectra of mesons and baryons. The calculations depicted in Figure 3 [18] use three adjustable parameters to fit the available proton and neutron form factor data. Two of these give the probabilities of higher Fock states (pion cloud contributions) for  $F_2(Q^2)$ , which, through comparison with data, are 30% (proton) and 40% (neutron). Departure of the third (parameter  $r$  Figure 3) from unity is interpreted as indicative of SU(6) spin-flavor symmetry breaking effects. The computed curves have an estimated accuracy of  $\approx 10\%$ , give a good account of the available  $G_E / G_M$  data for protons and neutrons (with  $r = 2.08$ ) and also describe a u/d flavor separation of  $F_1$  and  $F_2$  as performed in Ref. [20].

Note that, contrary to the DSE framework, LFHQCD predicts that  $\mu_n G_E^n / G_M^n$  rises towards an asymptotic value of  $\approx 0.85$ , rather than bending over and decreasing towards

zero. Such large differences in theoretical predictions emphasize the importance of collecting neutron data in the  $Q^2 \approx 4\text{--}10 \text{ (GeV/c)}^2$  region.

#### 2.4. The link with Generalized Parton Distributions

Generalized Parton Distributions (GPD) describe correlations between spatial and momentum degrees of freedom and permit the construction of various types of “3-D images” of the nucleon. The nucleon elastic form factors are critical to the experimental determination of GPDs [21]. In Deeply Virtual Compton Scattering (DVCS), which is generally held to be the optimum channel to access GPD information, the interference between Bethe Heitler and DVCS Handbag mechanisms is measured and the separation of these amplitudes requires EMFF information. The first moments of GPDs are related to the elastic form factors through model independent sum rules

$$\int_{-1}^{+1} dx H^q(x, \xi, Q^2) = F_1^q(Q^2) \quad \int_{-1}^{+1} dx E^q(x, \xi, Q^2) = F_2^q(Q^2). \quad (1)$$

These relations are currently some of the most important constraints on the forms of the GPD's and, since it is extremely unlikely that the GPDs will be mapped out exhaustively in the near future, constraints such as those in Equation 1 will be critical to extraction of GPD's. Already the constraints from those sum rules played an important role in the first estimates of nucleon quark angular momentum using the Ji Sum Rule and constraining GPDs is in itself is an excellent reason to experimentally determine the nucleon elastic form factors.

### 3. C-GEN Update and the Upcoming RP-GEN “proof-of-principle” Measurement

The design of this measurement followed that of the earlier 6 GeV era JLab E93-038 [15], which used the recoil polarimetry technique to measure  $G_E^n$  on a liquid deuterium target over a  $Q^2$  range of 0.45-1.45 (GeV/c)<sup>2</sup>. The present proposal extends that method by taking advantage of the full 11 GeV/c beam energy available in Hall C, a high-luminosity liquid deuterium target, and a significantly updated neutron polarimeter design with a higher figure of merit (FoM).

Following a short lull after the PAC37 approval (and the early stages of JLab's 12 GeV upgrade shutdown), the E12-11-009 Collaboration membership was reengaged, the Spokesperson list was refreshed, and we actively pursued the refinements and final details of the polarimeter design.

A GEANT4 simulation was written to cross check earlier FLUKA estimates and both the FoM and anticipated background rates were found to be consistent. The design of the E12-11-009 neutron polarimeter design was refined and the figure-of-merit (FoM) increased by roughly 10% over the initial plan. The scintillator bars, PMTs and supporting electronics were identified, and JLab designers were engaged to evaluate Hall layout and infrastructure requirements.

One important item that came out of the updated modeling and study was a recognition that the Charybdis magnet alone was likely insufficient to achieve the desired 4 T-m field. To this end, the Collaboration worked with JLab designers and management to identify two magnets that would satisfy the integrated field requirement. The first remained Charybdis, which is presently stored in the JLab Experimental Storage Building (ESB) and is in

excellent shape. The second was to be a BNL 48D48 magnet. That is the same type of magnet as is presently used in the Super BigBite (SBS) spectrometer. The enhanced detector design and Hall layout can be seen in Figure 4. As of 2016 a surplus 48D48 magnet had been identified at BNL, supporting power supplies were identified at JLab, and plans were underway to arrange for shipment. Depending on final scheduling and Hall availability, the (already on-site) SBS BNL 48D48 magnet is also an excellent option. (Given the projected experimental schedules for the SBS program and subsequent Moller experiment in Hall A, the SBS systems would likely be available to support a program in Hall C on a compatible timescale.)

Around that same period a new approach to extracting  $G_E^n$  from the  ${}^2H(\vec{e}, e'\vec{n})^1H$  reaction was also being explored. In PAC43 members of the SBS collaboration put forward LOI12-15-003 [6], which proposed taking advantage of several SBS detector systems, and focused on the  $np \rightarrow pn$  charge-exchange channel for recoil polarimetry. The PAC43 Final Report [22] highlighted the following Recommendation in response:

**Recommendation:** The proponents are encouraged to work with the lab management and the E12-11-009 collaboration to improve the FOM of the recoil neutron polarimeter in order to optimize the measurements using the already approved beam time of E12-11-009.

To address this, the SBS and C-GEN (E12-11-009) proponents of  $G_E^n/G_M^n$  by recoil-neutron polarimetry proposed a new “proof-of-principle” measurement at PAC45 that would simultaneously test *both* polarimetry techniques at a single  $Q^2$  of  $4.5 (\text{GeV}/c)^2$ . That measurement (E12-17-004) [7], referred to as *GEN-RP* was approved and will run concurrently with E12-09-019 [23] as part of the upcoming Super BigBite (SBS) run-group in Hall A beginning Fall of 2021.

Since that time, the majority of the Collaboration attention has been on developing and staging the RP-GEN measurement with the explicit plan to return to E12-11-009 with lessons-learned, and potentially important optimizations to the polarimeter. *Should the new charge-exchange channel demonstrate its promise, then the best path forward would be a new proposal in either Hall A or C using a redesigned polarimeter guided by what the RP-GEN collaboration learns.*

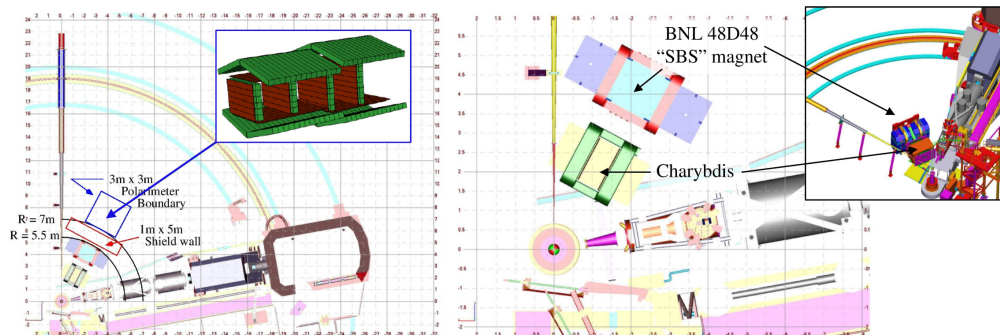


Figure 4: **Left:** Updated C-GEN polarimeter design (inset in upper-right), and location of principle polarimeter elements in Hall C. The electron arm is the SHMS to beam-left (not shown). **Right:** Updated C-GEN polarimeter magnet layout (Charybdis is near target, a BNL 48D48 is immediately downstream. Charybdis is presently in JLab’s Experimental Storage Building. A BNL 48D48 magnet is the foundation of the the Super BigBite (SBS) dipole.

### 3.1. “RP-Gen” (E12-17-004) Exploratory Measurement

Relatively recent data from JINR demonstrated that the  $np \rightarrow pn$  charge-exchange channel has a significant analyzing power, comparable to that of the more conventional  $np \rightarrow np$  approach at modest  $Q^2$ , but with a rapidly growing advantage at large  $Q^2$  where the forward-neutron  $np$  analyzing power falls off rapidly (Fig. 5). However, the practicality of this charge-exchange polarimetry technique is, as yet, unproven. The upcoming RP-Gen (E12-17-004) measurement [7] will address that issue head-on.

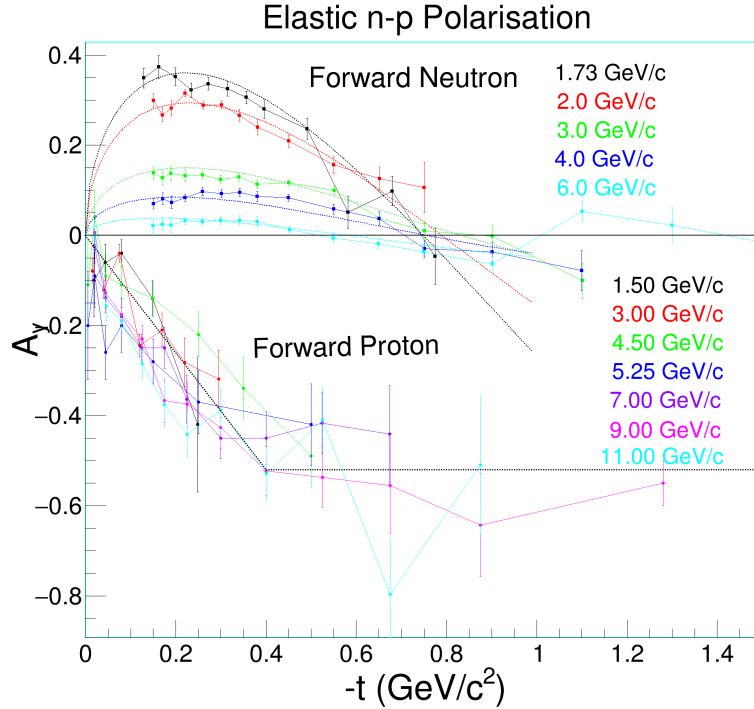


Figure 5: Top: the  $p_{lab}$  and  $t$ -dependence of the polarization of  $pn$  scattering [24, 25]. The smooth dotted lines show the fit of Ref. [26] to the  $pn$  data. Bottom: the  $p_{lab}$  and  $t$ -dependence of charge-exchange  $np$  scattering [27, 28].

The RP-Gen experiment is a relatively short (5 PAC day) addition to the SBS run-group that utilizes large portions of the existing BigBite and Super BigBite detector systems. BigBite will be the electron arm, and a neutron polarimeter composed of SBS, a hadron calorimeter (HCAL), GEM layers, scintillator based hodoscopes, and *two* neutron analyzers will be employed to simultaneously make two independent measurements of the ratio  $G_E^n/G_M^n$  using both the charge-exchange  $np \rightarrow pn$  technique *and* the more conventional  $np \rightarrow np$  polarimetry method. The most current details of the RP-Gen measurement may be found on the [E12-17-004 ERR Wiki](https://hallaweb.jlab.org/wiki/index.php/Gen-RP_Experiment_(E12-17-004))<sup>1</sup> page. Figures 6 and 7 show the floorplan for that measurement.

<sup>1</sup>[https://hallaweb.jlab.org/wiki/index.php/Gen-RP\\_Experiment\\_\(E12-17-004\)](https://hallaweb.jlab.org/wiki/index.php/Gen-RP_Experiment_(E12-17-004))

As noted in the RP-GEN proposal, and commended by the PAC45 Committee [29], that measurement will provide valuable information on the FoM for both reaction channels, and will be used to optimize the E12-11-009 polarimeter design. If the charge-exchange approach can be demonstrated to work as hoped, it will allow for powerful systemic cross-checks of the upcoming polarized  $^3\text{He}$  measurement of  $G_E^n$  out to  $Q^2$  of  $10 (\text{GeV}/c)^2$  using a recoil polarimetry approach. As the two approaches have quite different systematics and sensitivities to nuclear corrections, we believe measurements using both approaches are extremely valuable.

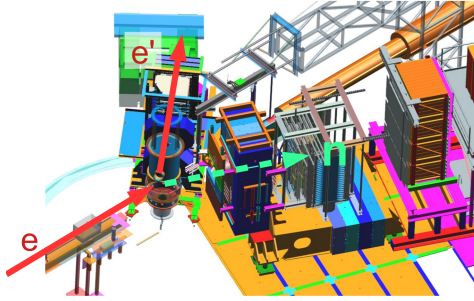


Figure 6: RP-GEN layout diagram in Hall A. BigBite is the the electron arm on beam-left. Super BigBite with a new neutron polarimeter detector stack and HCAL is on beam-right.

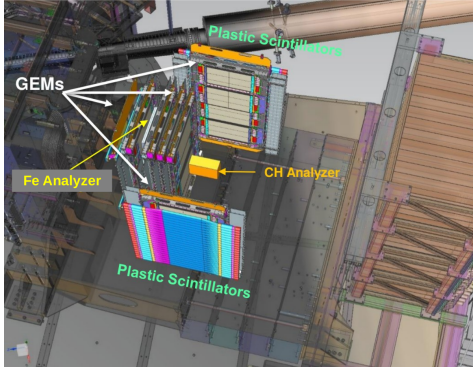


Figure 7: Rendering of the RP-GEN neutron polarimeter. The Fe analyzer is used to probe the charge-exchange reaction channel. The active CH analyzer is used to probe the conventional  $np \rightarrow np$  reaction channel.

#### 4. Summary

As outlined in Section 2 there is considerable interest and value in measuring the  $G_E^n/G_M^n$  ratio. The  $Q^2 > 3.5 (\text{GeV})^2$  region appears to have great sensitivity to a variety of theoretical models, yet remains largely unexplored. The first measurements in that region are expected to use the double polarization method on a polarized  $^3\text{He}$  target within the next few years. Regardless of the outcome, it is critical to have those measurements cross-checked using the recoil polarimetry method, a technique with very different nuclear corrections, backgrounds, and other systematic corrections.

There has been steady progress on the E12-11-009 C-GEN experimental development over the last 6–7 years. More recently, members of our Collaboration have joined forces with SBS Collaboration members to develop and run a short exploratory measurement as part of the upcoming SBS program in Hall A. However, executing the RP-GEN (E12-17-004) measurement is explicitly on the development path for the E12-11-009 C-GEN experiment.

We urge the PAC to reaffirm the importance of this measurement and maintain the 50 PAC days approved in PAC37 until the results of the RP-GEN measurement are clear. If the charge-exchange channel demonstrates its promise, then the best path forward would be a new proposal in either Hall A or C using a redesigned polarimeter guided by what the RP-GEN collaboration has learned.



## 5. References

- [1] The Neutron Electric Form Factor at  $Q^2$  up to 7 (GeV/c)<sup>2</sup> from the Reaction  ${}^2\text{H}(\vec{e}, e'\vec{n}){}^1\text{H}$  via Recoil Polarimetry, (JLab E12-11-009).  
URL <https://wiki.jlab.org/E12-11-009/images/6/6b/PR-11-009.pdf>
- [2] PAC37 Final Report (2011).  
URL [https://wiki.jlab.org/E12-11-009/images/5/52/PAC37\\_Report.pdf](https://wiki.jlab.org/E12-11-009/images/5/52/PAC37_Report.pdf)
- [3] S. Riordan, et al., Measurements of the Electric Form Factor of the Neutron  $Q^2=3.4$  GeV<sup>2</sup> Using the Reaction  ${}^3\text{He}(\vec{e}, e'n)pp$ , Phys. Rev. Lett. 105 (2010) 262302, (JLab E03-012). doi:10.1103/PhysRevLett.105.262302.
- [4] Measurement of the Neutron Electromagnetic Form Factor Ratio  $G_E^n/G_M^n$  at High  $Q^2$ , (JLab E12-09-016; Polarized  ${}^3\text{He}$  target).  
URL [http://www.jlab.org/exp\\_prog/proposals/09/PR12-09-016.pdf](http://www.jlab.org/exp_prog/proposals/09/PR12-09-016.pdf)
- [5] M. Jones, et al., Phys. Rev. Lett. 84 (2000) 1398.
- [6] Measurement of the Ratio  $G_E^n/G_M^n$  by the Double-polarized  ${}^2\text{H}(\vec{e}, e'\vec{n})$  Reaction, (JLab LOI12-15-003) (2015).  
URL [https://www.jlab.org/exp\\_prog/proposals/15/L0I12-15-003.pdf](https://www.jlab.org/exp_prog/proposals/15/L0I12-15-003.pdf)
- [7] J. Annand, V. Bellini, M. Kohl, N. Piskunov, B. Sawatzky, B. Wojtsekhowski, Measurement of the Ratio  $G_E^n/G_M^n$  by the Double-polarized  ${}^2\text{H}(\vec{e}, e'\vec{n})$  Reaction, (JLab E12-17-004).  
URL [http://www.jlab.org/exp\\_prog/proposals/09/PR12-09-019.pdf](http://www.jlab.org/exp_prog/proposals/09/PR12-09-019.pdf)
- [8] C. Roberts, A. Williams, Prog. Part. Nucl. Phys. 33 (1994) 477.
- [9] I. Cloët, et al., Few-Body Syst. 46 (2009) 1.
- [10] J. Segovia, et al., Few-Body Syst. 55 (2014) 1185.
- [11] O. Gayou, others, Phys. Rev. Lett. 88 (2002) 092301.
- [12] V. Punjabi, et al., Phys. Rev. C71 (2005) 055202.
- [13] A. Puckett, et al., Phys. Rev. Lett. 104 (2010) 242301.
- [14] A. Puckett, et al., Phys. Rev. C85 (2012) 045203.
- [15] B. Plaster, et al., Measurements of the Neutron Electric to Magnetic Form Factor Ratio  $G_E^n/G_M^n$  via the  ${}^2\text{H}(\vec{e}, e'\vec{n}){}^1\text{H}$  reaction to  $Q^2=1.45$  (GeV/c)<sup>2</sup>, Phys. Rev. C 73 (2006) 025205, (JLab 93-205). doi:10.1103/PhysRevC.73.025205.
- [16] J. Kelly, et al., Phys. Rev. C70 (2004) 068202.
- [17] D. Wilson, et al., Phys. Rev. C85 (2012) 025205.
- [18] R. Sufian, et al., Phys. Rev. D95 (2017) 014011.
- [19] I. Cloët, et al., Phys. Rev. C90 (2014) 045202.
- [20] I. Qattan, J. Arrington, Phys. Rev. C86 (2012) 065210.
- [21] M. Diehl, P. Kroll, Eur. J. Phys. C73 (2013) 2397.
- [22] PAC43 Final Report (2015).  
URL [https://www.jlab.org/exp\\_prog/PACpage/PAC43/PAC43\\_FINAL%20Report.pdf](https://www.jlab.org/exp_prog/PACpage/PAC43/PAC43_FINAL%20Report.pdf)
- [23] Precision Measurement of the Neutron Magnetic Form Factor up to  $Q^2=18.0$  (GeV/c)<sup>2</sup> by the Ratio Method, (JLab E12-09-019).  
URL [http://www.jlab.org/exp\\_prog/proposals/09/PR12-09-019.pdf](http://www.jlab.org/exp_prog/proposals/09/PR12-09-019.pdf)
- [24] R. Diebold, et al., Phys. Rev. Lett. 35 (1975) 632.
- [25] S. Kramer, et al., Phys. Rev. D17 (1978) 1709.
- [26] V. Ladygin, Analyzing Power of  $pp$  and  $np$  Elastic Scattering at Momenta between 2000 and 6000 MeV/c and Polarimetry at LHE, (Report E13-99-123) (1999).
- [27] P. Robrish, et al., Phys. Lett. B31 (1970) 617.
- [28] M. Abolins, et al., Phys. Rev. Lett. 30 (1973) 1183.
- [29] PAC45 Final Report (2017).  
URL [https://www.jlab.org/exp\\_prog/PACpage/PAC45/PAC45%20FINAL%20Report.pdf](https://www.jlab.org/exp_prog/PACpage/PAC45/PAC45%20FINAL%20Report.pdf)